International Journal of Mechanical, Industrial and Aerospace Sciences
ISSN: 2517-9950
Vol:7, No:5, 2013

Flexure of Cantilever Thick Beams Using Trigonometric Shear Deformation Theory

Yuwaraj M. Ghugal, Ajay G. Dahake

Abstract**—**A trigonometric shear deformation theory for flexure of thick beams, taking into account transverse shear deformation effects, is developed. The number of variables in the present theory is same as that in the first order shear deformation theory. The sinusoidal function is used in displacement field in terms of thickness coordinate to represent the shear deformation effects. The noteworthy feature of this theory is that the transverse shear stresses can be obtained directly from the use of constitutive relations with excellent accuracy, satisfying the shear stress free conditions on the top and bottom surfaces of the beam. Hence, the theory obviates the need of shear correction factor. Governing differential equations and boundary conditions are obtained by using the principle of virtual work. The thick cantilever isotropic beams are considered for the numerical studies to demonstrate the efficiency of the. Results obtained are discussed critically with those of other theories.

Keywords**—**Trigonometric shear deformation, thick beam, flexure, principle of virtual work, equilibrium equations, stress.

I. Introduction

IT is well-known that elementary theory of bending of beam based on Euler-Bernoulli hypothesis disregards the effects of the shear deformation and stress concentration. The theory is suitable for slender beams and is not suitable for thick or deep beams since it is based on the assumption that the transverse normal to neutral axis remains so during bending and after bending, implying that the transverse shear strain is zero. Since theory neglects the transverse shear deformation, it underestimates deflections in case of thick beams where shear deformation effects are significant.

Bresse [1], Rayleigh [2], and Timoshenko [3] were the pioneer investigators to include refined effects such as rotatory inertia and shear deformation in the beam theory. Timoshenko showed that the effect of transverse vibration of prismatic bars. This theory is now widely referred to as Timoshenko beam theory or first order shear deformation theory (FSDT) in the literature. In this theory transverse shear strain distribution is assumed to be constant through the beam thickness and thus requires shear correction factor to appropriately represent the strain energy of deformation. Cowper [4] has given refined expression for the shear correction factor for different cross-sections of beam. The accuracy of Timoshenko beam theory for transverse vibrations of simply supported beam in respect of the fundamental frequency is verified by Cowper [5] with a plane stress exact elasticity solution. To remove the discrepancies in classical and first order shear deformation theories, higher order or refined shear deformation theories were developed and are available in the open literature for static and vibration analysis of beam.

Levinson [6], Bickford [7], Rehfield and Murty [8], Krishna Murty [9], Baluch, Azad and Khidir [10], Bhimaraddi and Chandrashekhara [11] presented parabolic shear deformation theories assuming a higher variation of axial displacement in terms of thickness coordinate. These theories satisfy shear stress free boundary conditions on top and bottom surfaces of beam and thus obviate the need of shear correction factor. Irretier [12] studied the refined dynamical effects in linear, homogenous beam according to theories, which exceed the limits of the Euler-Bernoulli beam theory. These effects are rotary inertia, shear deformation, rotary inertia and shear deformation, axial pre-stress, twist and coupling between bending and torsion.

Kant and Gupta [13], Heyliger and Reddy [14] presented finite element models based on higher order shear deformation uniform rectangular beams. However, these displacement based finite element models are not free from phenomenon of shear locking (Averill and Reddy [15], Reddy [16]).

There is another class of refined theories, which includes trigonometric functions to represent the shear deformation effects through the thickness. Vlasov and Leont'ev [17], Stein [18] developed refined shear deformation theories for thick beams including sinusoidal function in terms of thickness coordinate in displacement field. However, with these theories shear stress free boundary conditions are not satisfied at top and bottom surfaces of the beam. Ghugal and Sharma [19] presented hyperbolic shear deformation theory for flexure and vibration of thick isotropic beams. A study of literature by Ghugal and Shimpi [20] indicates that the research work dealing with flexural analysis of thick beams using refined trigonometric and hyperbolic shear deformation theories is very scarce and is still in infancy. In this paper development of theory and its application to thick cantilever beams is presented.

II. Development of Theory

The beam under consideration as shown in Fig. 1 occupies in $0 - x - y - z$ Cartesian coordinate system the region:

$$0 \le x \le L \; ; \quad 0 \le y \le b \; ; \quad -\frac{h}{2} \le z \le \frac{h}{2}$$

where x, y, z are Cartesian coordinates, L and b are the length and width of beam in the x and y directions respectively, and h

Yuwaraj M. Ghugal is Professor at the Applied Mechanics Department, Government Engineering College, Karad, Maharashtra, India (phone: 09370353722; e-mail: ghugal@ rediffmail.com).

Ajay G. Dahake is Research Scholar at the Applied Mechanics Department, Government Engineering College, Aurangabad, Maharashtra, India (phone: 08149409975; e-mail: ajaydahake@ gmail.com).

is the thickness of the beam in the z-direction. The beam is made up of homogeneous, linearly elastic isotropic material.

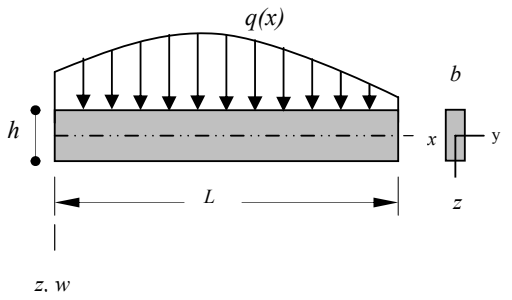

Fig. 1 Beam under bending in *x*-*z* plane

A. The Displacement Field

The displacement field of the present beam theory is of the form:

$$u(x,z) = -z\frac{dw}{dx} + \frac{h}{\pi}\sin\frac{\pi z}{h}\phi(x)$$
$$w(x,z) = w(x) \quad (1)$$

where u is the axial displacement in x direction and w is the transverse displacement in z direction of the beam. The sinusoidal function is assigned according to the shear stress distribution through the thickness of the beam. The function ϕ represents rotation of the beam at neutral axis, which is an unknown function to be determined. The normal and shear strains obtained within the framework of linear theory of elasticity using displacement field given by (1) are as follows.

$$\text{Normal strain: } \varepsilon_x = \frac{\partial u}{\partial x} = -z\frac{d^2w}{dx^2} + \frac{h}{\pi}\sin\frac{\pi z}{h}\frac{d\phi}{dx} \quad (2)$$

$$\text{Shear strain: } \gamma_{zx} = \frac{\partial u}{\partial z} + \frac{dw}{dx} = \cos\frac{\pi z}{h}\phi \quad (3)$$

The stress-strain relationships used are as follows:

$$\sigma_x = E\varepsilon_x,\ \tau_{zx} = G\gamma_{zx} \quad (4)$$

B. Governing Equations and Boundary Conditions

Using (2) through (4) and using the principle of virtual work, variationally consistent governing differential equations and boundary conditions for the beam under consideration can be obtained. The principle of virtual work when applied to the beam leads to:

$$b\int_{x=0}^{x=L}\int_{z=-h/2}^{z=+h/2}\left(\sigma_x\delta\varepsilon_x + \tau_{zx}\delta\gamma_{zx}\right)dx\,dz - \int_{x=0}^{x=L} q(x)\,\delta w\,dx = 0 \quad (5)$$

where the symbol δ denotes the variational operator. Employing Green's theorem to (4) successively, we obtain the coupled Euler-Lagrange equations which are the governing differential equations and associated boundary conditions of the beam. The governing differential equations obtained are as follows:

$$EI\frac{d^4w}{dx^4} - \frac{24}{\pi^3}EI\frac{d^3\phi}{dx^3} = q(x) \quad (6)$$

$$\frac{24}{\pi^3}EI\frac{d^3w}{dx^3} - \frac{6}{\pi^2}EI\frac{d^2\phi}{dx^2} + \frac{GA}{2}\phi = 0 \quad (7)$$

The associated consistent natural boundary conditions obtained are of following form:

At the ends $x = 0$ and $x = L$

$$V_x = EI\frac{d^3w}{dx^3} - \frac{24}{\pi^3}EI\frac{d^2\phi}{dx^2} = 0 \text{ or } w \text{ is prescribed} \quad (8)$$

$$M_x = EI\frac{d^2w}{dx^2} - \frac{24}{\pi^3}EI\frac{d\phi}{dx} = 0 \text{ or } \frac{dw}{dx} \text{ is prescribed} \quad (9)$$

$$M_a = EI\frac{24}{\pi^3}\frac{d^2w}{dx^2} - \frac{6}{\pi^2}EI\frac{d\phi}{dx} = 0 \text{ or } \phi \text{ is prescribed} \quad (10)$$

Thus the boundary value problem of the beam bending is given by the above variationally consistent governing differential equations and boundary conditions.

C. The General Solution of Governing Equilibrium Equations of the Beam

The general solution for transverse displacement $w(x)$ and warping function $\phi(x)$ is obtained using (6) and (7) using method of solution of linear differential equations with constant coefficients. Integrating and rearranging (6), we obtain the following expression

$$\frac{d^3w}{dx^3} = \frac{24}{\pi^3}\frac{d^2\phi}{dx^2} + \frac{Q(x)}{EI} \quad (11)$$

where $Q(x)$ is the generalized shear force for beam and it is given by $Q(x) = \int_0^x q\,dx + C_1$.

Now (7) is rearranged in the following form:

$$\frac{d^3w}{dx^3} = \frac{\pi}{4}\frac{d^2\phi}{dx^2} - \beta\phi \quad (12)$$

A single equation in terms of ϕ is now obtained using (11) and (12) as:

$$\frac{d^2\phi}{dx^2} - \lambda^2\phi = \frac{Q(x)}{\alpha EI} \quad (13)$$

where constants α, β and λ in (12) and (13) are as follows

$$\alpha = \left(\frac{\pi}{4} - \frac{24}{\pi^3}\right),\ \beta = \left(\frac{\pi^3}{48}\frac{GA}{EI}\right) \text{and } \lambda^2 = \frac{\beta}{\alpha}$$

The general solution of (13) is as follows:

$$\phi(x) = C_2 \cosh \lambda x + C_3 \sinh \lambda x - \frac{Q(x)}{\beta EI} \tag{14}$$

The equation of transverse displacement $w(x)$ is obtained by substituting the expression of $\phi(x)$ in (12) and then integrating it thrice with respect to x. The general solution for $w(x)$ is obtained as follows:

$$EI\, w(x) = \iiiint q\, dx\, dx\, dx\, dx + \frac{C_1 x^3}{6} + \left(\frac{\pi}{4}\lambda^2 - \beta\right)\frac{EI}{\lambda^3} \left(C_2 \sinh\lambda x + C_3 \cosh\lambda x\right) + C_4 \frac{x^2}{2} + C_5 x + C_6 \tag{15}$$

where C_1, C_2, C_3, C_4, C_5 and C_6 are arbitrary constants and can be obtained by imposing boundary conditions of beam.

III. Illustrative Examples

In order to prove the efficacy of the present theory, the following numerical examples are considered. The following material properties for beam are used

$$E = 210 \text{ GPa}, \mu = 0.3 \text{ and } \rho = 7800 \text{ kg/m}^3,$$

where E is the Young's modulus, ρ is the density, and μ is the Poisson's Units

A. Example 1: Cantilever Beam with Varying Load

The beam has its origin at left hand side fixed support at x = 0 and free at $x = L$. The beam is subjected to varying load, on surface $z = +h/2$ acting in the downward z direction with maximum intensity of load q_0.

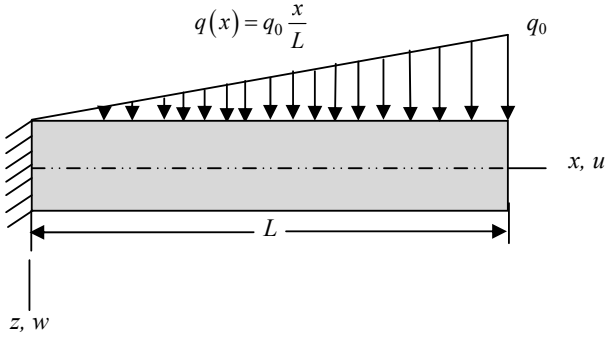

Fig. 2 Cantilever beam with varying load

General expressions obtained for $w(x)$ and $\phi(x)$ are as follows:

$$w(x) = \frac{q_0 L^4}{120EI}\left\{\frac{x^5}{L^5} - 10\frac{x^3}{L^3} + 20\frac{x^2}{L^2} + 6\frac{E}{G}\frac{h^2}{L^2}\left[\left(\frac{x}{L} + \frac{(\zeta(x)-1)}{\lambda L}\right) - \frac{x^2}{L^2}\right]\right\} \tag{16}$$

$$\phi(x) = \frac{q_0 L}{2\beta EI}\left(1 + \zeta(x) - \frac{x^2}{L^2}\right) \tag{17}$$

where $\zeta(x) = (\sinh \lambda x - \cosh \lambda x)$

$$u = \frac{q_0 h}{Eb}\left\{\begin{array}{l} -\frac{z}{h}\frac{L^3}{h^3}\left[\frac{1}{2}\frac{x^4}{L^4} - 3\frac{x^2}{L^2} + 4\frac{x}{L} + \right. \\ \left. \frac{6}{5}\frac{E}{G}\frac{h^2}{L^2}\left(1 + \zeta(x) - 2\frac{x}{L}\right)\right] \\ +\frac{16}{\pi^4}\frac{E}{G}\frac{L}{h}\sin\frac{\pi z}{\mathrm{h}}\left(1 - \frac{x^2}{L^2} + \zeta(x)\right) \end{array}\right\} \tag{18}$$

$$\sigma_x = \frac{q_0}{b}\left\{\begin{array}{l} -\frac{z}{h}\left[\frac{L^2}{h^2}\left(4 - 6\frac{x}{L} + 2\frac{x^3}{L^3}\right)\right. \\ \left. -\frac{6}{5}\frac{E}{G}\left(\frac{1}{2} + \lambda L\,\zeta(x)\right)\right] \\ -\frac{24}{\pi^4}\frac{E}{G}\sin\frac{\pi z}{h}\left(2\frac{x}{L} + \lambda L\,\zeta(x)\right) \end{array}\right\} \tag{19}$$

$$\tau_{zx} = \frac{24}{\pi^3}\frac{q_0}{b}\frac{L}{h}\cos\frac{\pi z}{h}\left(1 - \frac{x^2}{L^2} + \zeta(x)\right) \tag{20}$$

$$\tau_{zx} = 3\frac{q_0 L}{bh}\left\{\begin{array}{l} \left[\frac{z^2}{h^2} - \frac{1}{4}\right]\left[\frac{1}{4}\frac{x^2}{L^2} + \frac{1}{4}\frac{x}{L} - \frac{1}{2\pi^2}\frac{E}{G}\frac{h^2}{L^2}\right. \\ \left. +\frac{24}{\pi^6}\frac{E}{G}\frac{h^2}{L^2}\left(\lambda^2 L^2\right)\zeta(x)\right] \\ +\frac{8}{\pi^5}\frac{E}{G}\frac{h^2}{L^2}\cos\frac{\pi z}{h}\left[\left(\lambda^2 L^2\right)\zeta(x) - 2\right] \end{array}\right\} \tag{21}$$

B. Example 2: Cantilever Beam with Parabolic Load

The beam has its origin at left hand side fixed support at x = 0 and free at $x = L$. The beam is subjected to parabolic load, on surface $z = +h/2$ acting in the downward z direction with maximum intensity of load q_0.

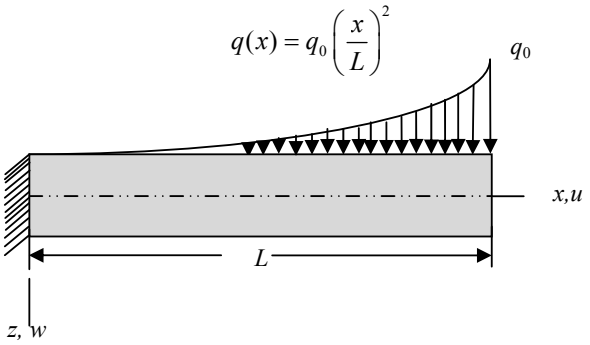

Fig. 3 Cantilever beam with parabolic load

General expressions obtained for $w(x)$ and $\phi(x)$ are as follows:

$$w(x)=\frac{q_0L^4}{360EI}\left\{\begin{array}{l}\left(\frac{x^6}{L^6}-20\frac{x^3}{L^3}+45\frac{x^2}{L^2}\right)\\ +12\frac{E}{G}\frac{h^2}{L^2}\left(\frac{x}{L}+\frac{(-1-\zeta(x))}{\lambda L}\right)\end{array}\right\} \tag{22}$$

$$\phi(x)=\frac{q_0L}{3\beta EI}\left(1-\frac{x^3}{L^3}+\zeta(x)\right) \tag{23}$$

The axial displacement and stresses obtained based on above solutions are as follows

$$u=\frac{q_0h}{Eb}\left\{\begin{array}{l}-\frac{z}{h}\frac{L^3}{h^3}\left[\frac{1}{5}\frac{x^5}{L^5}-2\frac{x^2}{L^2}+3\frac{x}{L}+\frac{2}{5}\frac{E}{G}\frac{h^2}{L^2}(1+\zeta(x))\right]\\ +\frac{16}{\pi^4}\frac{E}{G}\frac{L}{h}\sin\frac{\pi z}{\mathrm{h}}\left(1-\frac{x^3}{L^3}+\zeta(x)\right)\end{array}\right\} \tag{24}$$

$$\sigma_x=\frac{q_0}{b}\left\{\begin{array}{l}-\frac{z}{h}\left[\frac{L^2}{h^2}\left(\frac{x^4}{L^4}-4\frac{x}{L}+3\right)+\frac{2}{5}\frac{E}{G}[\lambda L\,\zeta(x)]\right]\\ +\frac{16}{\pi^4}\frac{E}{G}\sin\frac{\pi z}{h}\left(-3\frac{x^2}{L^2}-\lambda L\zeta(x)\right)\end{array}\right\} \tag{25}$$

$$\tau_{zx}^{CR}=\frac{16}{\pi^3}\frac{q_0}{b}\frac{L}{h}\cos\frac{\pi z}{h}\left(1-\frac{x^3}{L^3}+\zeta(x)\right) \tag{26}$$

$$\tau_{zx}^{EE}=2\frac{q_0L}{bh}\left\{\begin{array}{l}\left[\frac{z^2}{h^2}-\frac{1}{4}\right]\left[\frac{x^3}{L^3}-1+\frac{1}{10}\frac{E}{G}\frac{h^2}{L^2}\left(\lambda^2L^2\right)\zeta(x)\right]\\ +\frac{8}{\pi^5}\frac{E}{G}\frac{h^2}{L^2}\cos\frac{\pi z}{h}\left(-6\frac{x}{L}+\left(\lambda^2L^2\right)\zeta(x)\right)\end{array}\right\} \tag{27}$$

IV. Numerical Results

In this paper, the results for inplane displacement, transverse displacement, inplane and transverse stresses are presented in the following non dimensional form for the purpose of presenting the results in this work.

For beams subjected to various load, q(x);

$$\bar{u}=\frac{Ebu}{q_0h},\quad \bar{w}=\frac{10Ebh^3w}{q_0L^4},$$
$$\bar{\sigma}_x=\frac{b\sigma_x}{q_0},\quad \bar{\tau}_{zx}=\frac{b\tau_{zx}}{q_0}$$

TABLE I
Non-Dimensional Axial Displacement ($\bar{u}$) at (x = 0.25L, z = h/2), Transverse Deflection ($\bar{w}$) at (x = 0.25L, z =0.0) Axial Stress ($\bar{\sigma}_x$) at (x =0.25L, z = h/2) Maximum Transverse Shear Stresses $\bar{\tau}_{zx}^{CR}$ and $\bar{\tau}_{zx}^{EE}$ at (x = 0, z = 0) of the Beam Subjected to Varying Load for Aspect Ratio S = 4 and 10 (Example 1)

Model	S	$\bar{u}$	$\bar{w}$	$\bar{\sigma}_x$	$\bar{\tau}_{zx}^{CR}$	$\bar{\tau}_{zx}^{EE}$
TSDT		54.2767	12.6172	42.5408	1.4763	-2.5000
HPSDT		54.2637	12.6187	44.8793	1.7439	-3.4132
HSDT	4	54.2771	12.6191	42.9385	1.5394	-2.1287
FSDT		48.0000	11.3250	32.0000	0.9772	3.000
ETB		48.0000	11.0000	32.0000	—	3.000
TSDT		765.6917	11.2601	223.9812	6.2077	2.7248
HPSDT		765.6593	11.2600	229.8401	6.6373	3.1864
HSDT	10	765.6928	11.2603	233.2660	6.2594	3.1465
FSDT		750.0000	11.0520	200.0000	1.5373	7.500
ETB		750.0000	11.0000	200.0000	—	7.500

TABLE II
Non-Dimensional Axial Displacement ($\bar{u}$) at (x = 0.25L, z = h/2), Transverse Deflection ($\bar{w}$) at (x = 0.25L, z =0.0) Axial Stress ($\bar{\sigma}_x$) at (x =0.25L, z = h/2) Maximum Transverse Shear Stresses $\bar{\tau}_{zx}^{CR}$ and $\bar{\tau}_{zx}^{EE}$ at (x = 0.01L, z = 0) of the Beam Subjected to Parabolic Load for Aspect Ratio S = 4 and 10 (Example 2)

Model	S	$\bar{u}$	$\bar{w}$	$\bar{\sigma}_x$	$\bar{\tau}_{zx}^{CR}$	$\bar{\tau}_{zx}^{EE}$
TSDT		44.6919	10.1289	31.5541	0.9843	-1.3644
HPSDT		48,8646	10.9468	34.6825	1.1627	-2.2786
HSDT	4	48.8990	10.9519	33.3971	1.0264	-1.4190
FSDT		38.4000	8.8291	24.0000	0.7335	1.9999
ETB		38.4000	8.6667	24.0000	—	1.9999
TSDT		615.7298	8.9015	166.5143	4.1390	1.8179
HPSDT		626.1615	9.0322	171.9896	4.4253	2.1254
HSDT	10	626.2476	9.0331	168.7571	4.1735	2.0981
FSDT		600.0000	8.6926	150.0000	1.1530	5.0000
ETB		600.0000	8.6667	150.0000	—	5.0000

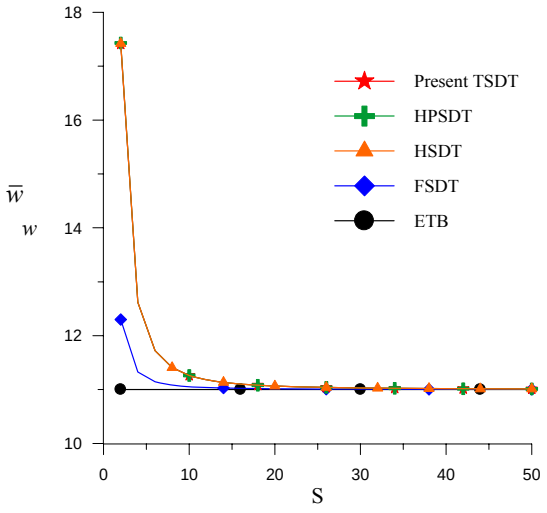

Fig. 4 Variation of maximum transverse displacement ($\bar{w}$) of beam at ($x = L$, $z = 0$) when subjected to varying load with aspect ratio S (Example 1)

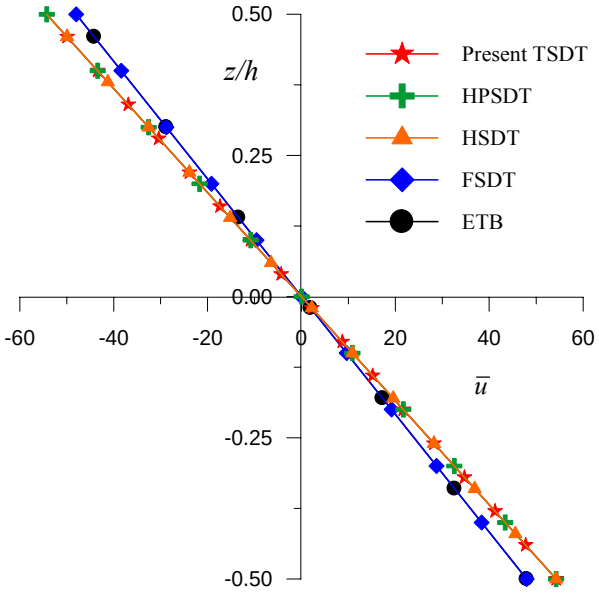

Fig. 5 Variation of axial displacement ($\bar{u}$) through the thickness of beam at ($x = L, z$) when subjected to varying load for aspect ratio 4 (Example 1)

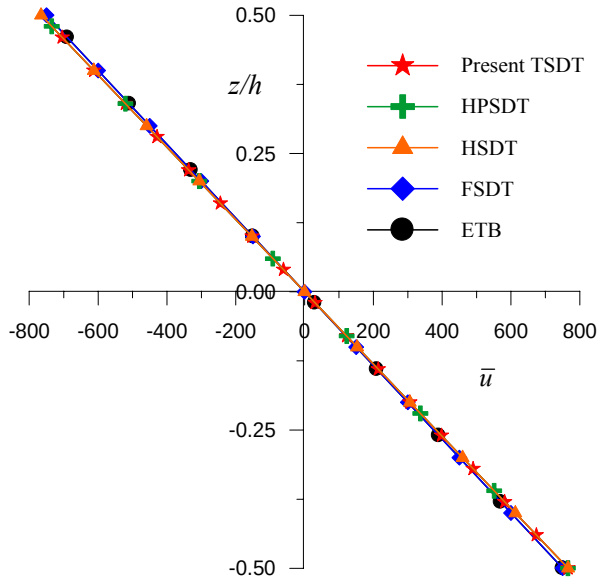

Fig. 6 Variation of axial displacement ($\bar{u}$) through the thickness of beam at ($x = L, z$) when subjected to varying load for aspect ratio 10 (Example 1)

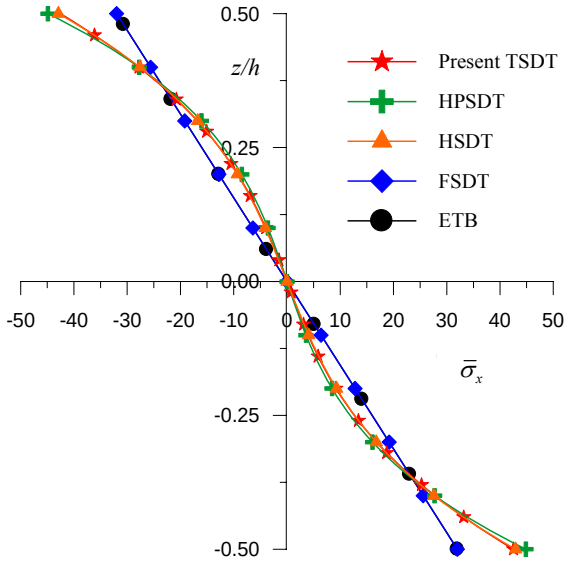

Fig. 7 Variation of axial stress ($\bar{\sigma}_x$) through the thickness of beam at ($x = 0, z$) when subjected to varying load for aspect ratio 4 (Example 1)

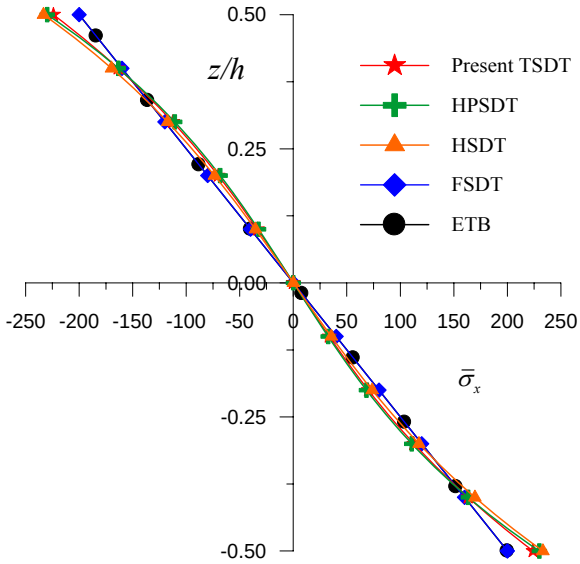

Fig. 8 Variation of axial stress ($\bar{\sigma}_x$) through the thickness of beam at ($x = 0, z$) when subjected to varying load for aspect ratio 10. (Example 1)

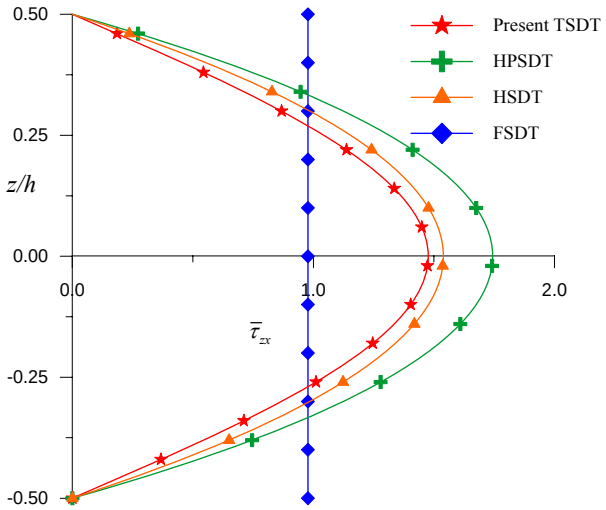

Fig. 9 Variation of transverse shear stress ($\overline{\tau}_{zx}$) through the thickness of beam at ($x = 0.01L$, z) when subjected to varying load and obtain via constitutive relation for aspect ratio 4 (Example 1)

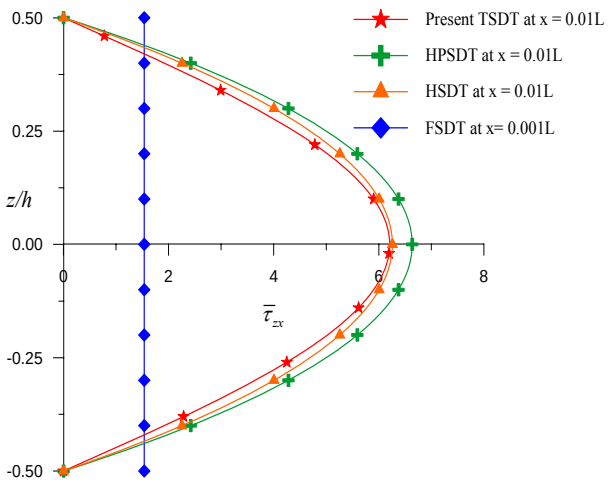

Fig. 10 Variation of transverse shear stress ($\overline{\tau}_{zx}$) through the thickness of beam at ($x = 0.01L$, z) when subjected to varying load and obtain via constitutive relation for aspect ratio 10 (Example 1)

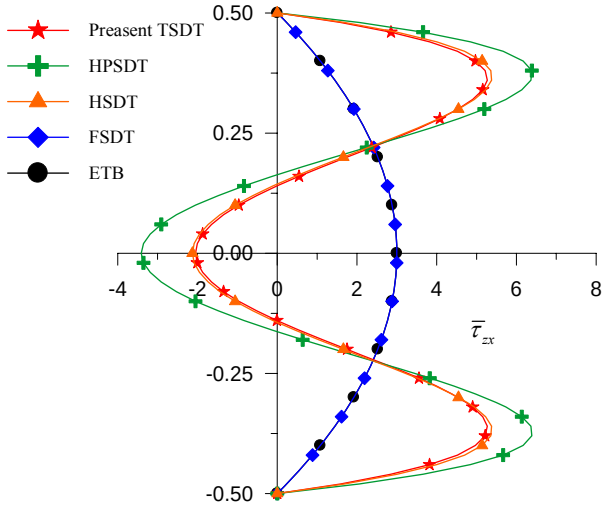

Fig. 11 Variation of transverse shear stress ($\overline{\tau}_{zx}$) through the thickness of beam at ($x = 0$, z) when subjected to varying load and obtain using equilibrium equation for aspect ratio 4 (Example 1)

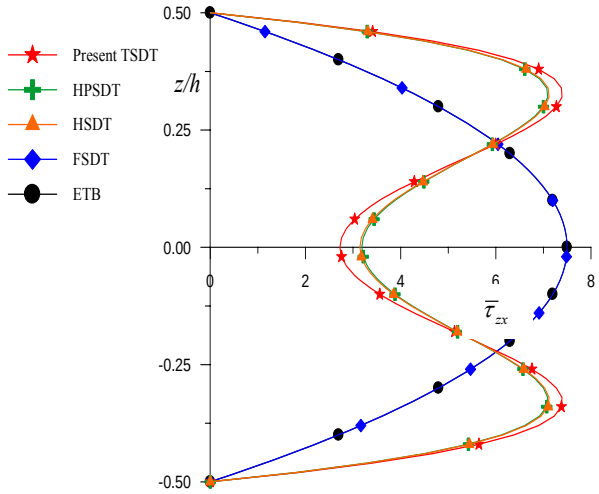

Fig. 12 Variation of transverse shear stress ($\overline{\tau}_{zx}$) through the thickness of beam at ($x = 0$, z) when subjected to varying load and obtain using equilibrium equation for aspect ratio 10 (Example 1)

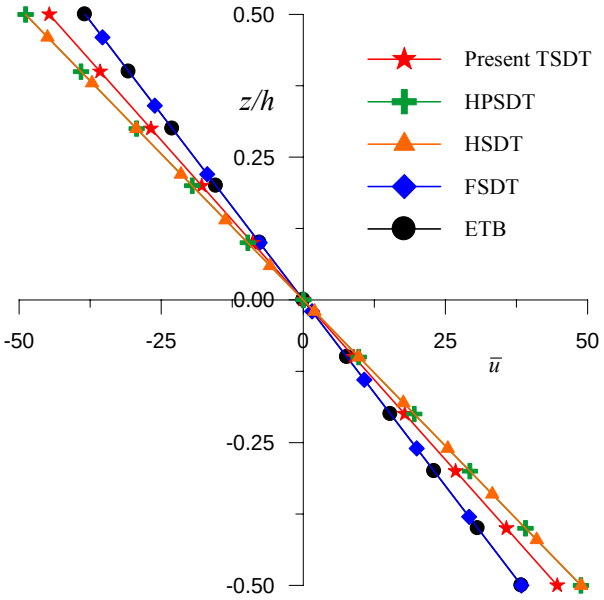

Fig. 13 Variation of axial displacement ($\bar{u}$) through the thickness of beam at ($x = L, z$) when subjected to parabolic load for aspect ratio 4 (Example 2)

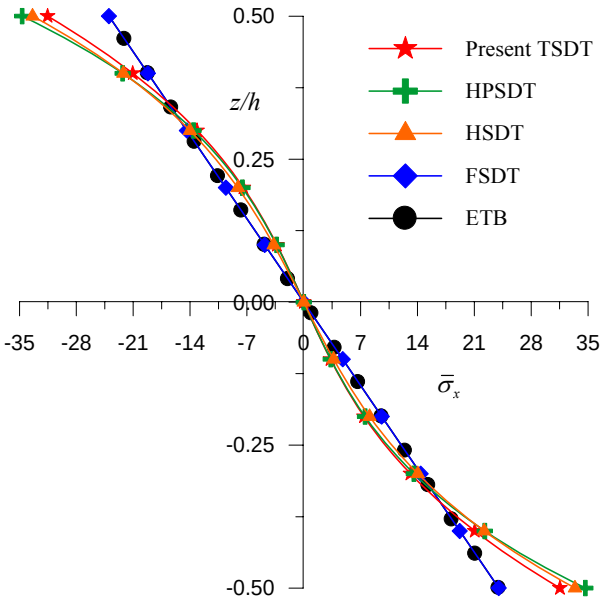

Fig. 15 Variation of axial stress ($\bar{\sigma}_x$) through the thickness of beam at ($x = 0, z$) when subjected to parabolic load for aspect ratio 4 (Example 2)

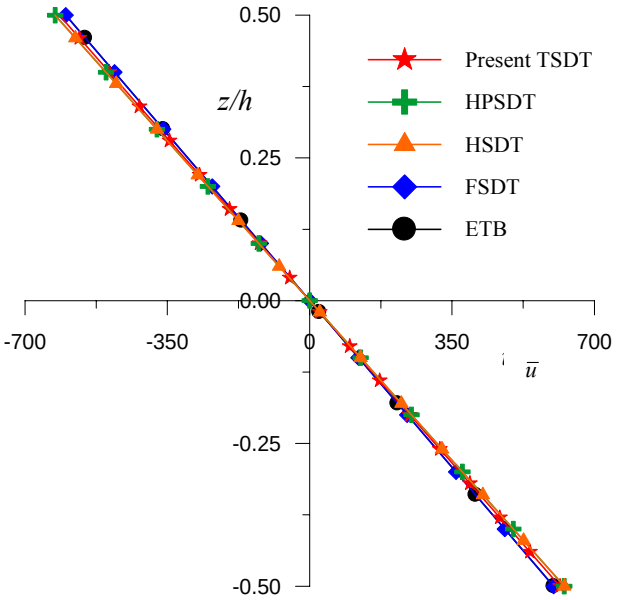

Fig. 14 Variation of axial displacement ($\bar{u}$) through the thickness of beam at ($x = L, z$) when subjected to parabolic load for aspect ratio 10 (Example 2)

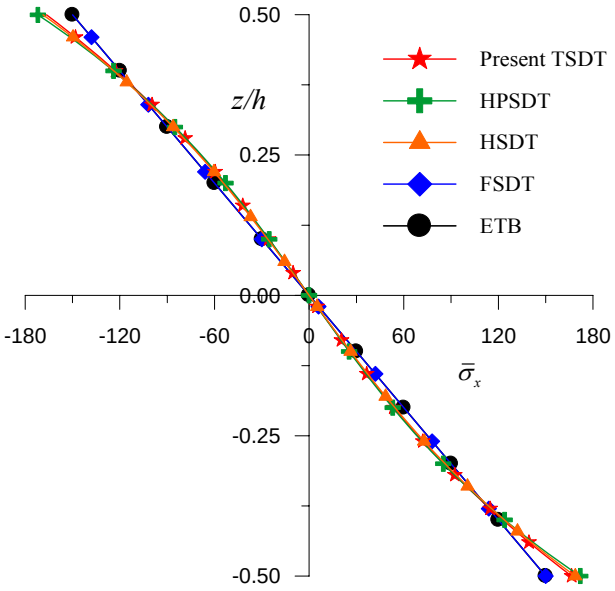

Fig. 16 Variation of axial stress ($\bar{\sigma}_x$) through the thickness of beam at ($x = 0, z$) when subjected to parabolic load for aspect ratio 10 (Example 2)

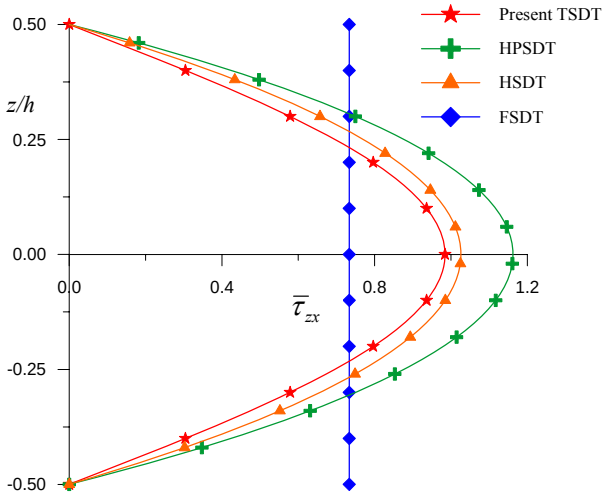

Fig. 17 Variation of transverse shear stress ($\overline{\tau}_{zx}$) through the thickness of beam at ($x = 0.01L$, z) when subjected to parabolic load and obtain via constitutive relation for aspect ratio 4 (Example 2)

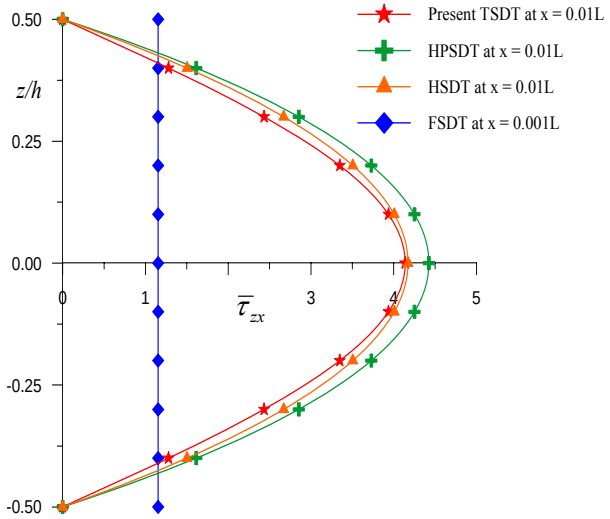

Fig. 18 Variation of transverse shear stress ($\overline{\tau}_{zx}$) through the thickness of beam at ($x = \alpha L$, z) when subjected to parabolic load and obtain via constitutive relation for aspect ratio 10 (Example 2)

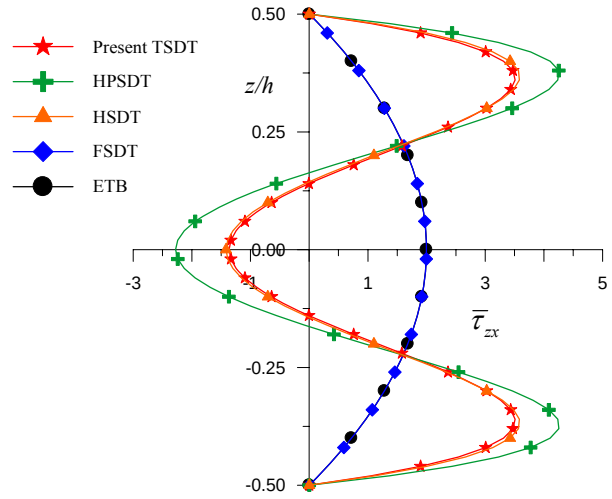

Fig. 19 Variation of transverse shear stress ($\overline{\tau}_{zx}$) through the thickness of beam at ($x = 0$, z) when subjected to parabolic load and obtain using equilibrium equation for aspect ratio 4 (Example 2)

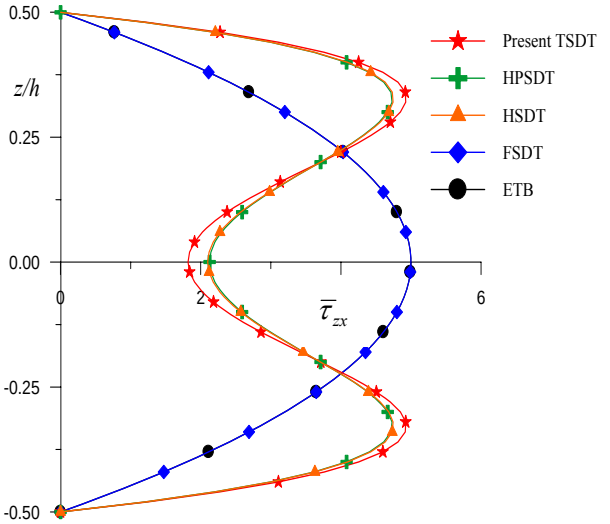

Fig. 20 Variation of transverse shear stress ($\overline{\tau}_{zx}$) through the thickness of beam at ($x = 0$, z) when subjected to parabolic load and obtain using equilibrium equation for aspect ratio 10 (Example 2)

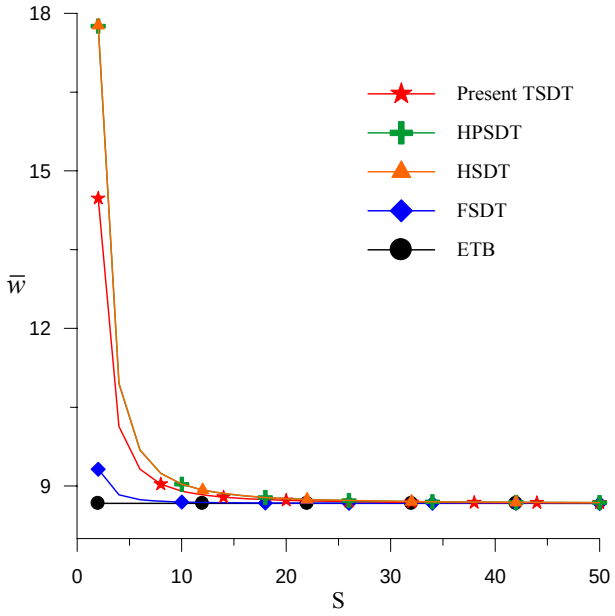

Fig. 21 Variation of maximum transverse displacement ($\bar{w}$) of beam at ($x = L, z = 0$) when subjected to parabolic load with aspect ratio S. (Example 2)

V. Discussion of Results

The comparison of results of maximum non-dimensional axial displacement ($\bar{u}$) for the aspect ratios of 4 and 10 is presented in Tables I and II for beams subjected to linearly varying and parabolic load (see Figs. 2 and 3). Among the results of all the other theories, the values of axial displacement given by present theory are in close agreement with the values of other refined theories for aspect ratio 4 and 10.The through thickness distribution of this displacement obtained by present theory is in close agreement with other refined theories except the one given by classical and first order shear deformation theory (FSDT) as shown in Figs. 5, 6, 13, and 14 for aspect ratio 4 and 10.

The comparison of results of maximum non-dimensional transverse displacement ($\bar{w}$) for the aspect ratios of 4 and 10 is presented in Tables I and II for beams subjected to linearly varying load and parabolic load. Among the results of all the other theories, the values of present theory are in excellent agreement with the values of other refined theories for aspect ratio 4 and 10 except those of classical beam theory (ETB) and FSDT of Timoshenko. The variation of $\bar{w}$ with aspect ratio (S) is shown in Figs. 4 and 21. For the aspect ratios greater than 20 all the refined theories converges to the values of classical beam theory.

The results of axial stress ($\bar{\sigma}_x$) are shown in Tables I and II 4 for aspect ratios 4 and 10. The axial stresses given by present theory are compared with other higher order shear deformation theories. It is observed that the results by present theory are in excellent agreement with other refined theories. However, ETB and FSDT yield lower values of this stress as compared to the values given by other refined theories. The through the thickness variation of this stress given by ETB and FSDT is linear. Present and other higher order refined theories provide the non-linear variations of axial stress across the thickness at the built-in end due to heavy stress concentration. However, this effect of local stress concentration cannot be captured by lower order theories such as ETB and FSDT. The variations of this stress are shown in Figs. 7, 8, 15 and 16.

The transverse shear stresses ($\bar{\tau}_{zx}$) are obtained directly by constitutive relation and, alternatively, by integration of equilibrium equation of two dimensional elasticity and are denoted by ($\bar{\tau}_{zx}^{CR}$) and ($\bar{\tau}_{zx}^{EE}$) respectively. The transverse shear stress satisfies the stress free boundary conditions on the top $\left(z = -h/2\right)$ and bottom $\left(z = +h/2\right)$ surfaces of the beam when these stresses are obtained by both the above mentioned approaches. The comparison of maximum non-dimensional transverse shear stress for a cantilever beam with varying load obtained by the present theory and other refined theories is presented in Tables I and II for aspect ratio of 4 and 10 respectively. The maximum transverse shear stress obtained by present theory using constitutive relation is in good agreement with that of higher order theory (HSDT), however HPSDT shows little departure from these theories for aspect ratio 4 and for aspect ratio 10 results of present theory and HSDT are in excellent agreement with each other. Among the values of this stress, the values obtained by HPSDT using equilibrium equation show considerable departure from the values of present and HSDT. The values of present theory and those of HSDT are in good agreement with each other. The through thickness variation of this stress obtained via constitutive relation are presented graphically in Figs. 9, 10, 16, 17 and those obtained via equilibrium equation are presented in Figs. 11, 12, 19 and 20. It can be seen from these figures that the nature of variation obtained by both the approaches is different from each other.

The through thickness variation of this stress via equilibrium equation shows the anomalous behavior (changes its sign) due to heavy stress concentration associated with the built-in end of the beam. The maximum value of this stress does not occur at the neutral axis, however, it is observed to be shifted at $z = 0.375h$. Such a behavior is also observed by Hildebrand and Reissner [21]. The ETB and FSDT yield the identical values this stress at $z = 0$ and the variations across the thickness of the beam. It is seen that the anomalous behavior in the vicinity of built-in end cannot be captured by constitutive relation. Further, lower order theories, ETB and FSDT, cannot predict this behavior even with the use of equilibrium equation. Hence, the use of higher order or equivalent shear deformation theories is necessary to recover the effects of stress concentration at the built-in end of the beam with the use of equilibrium equation of two-dimensional theory of elasticity.

VI. Conclusion

The variationally consistent theoretical formulation of the theory with general solution technique of governing

differential equations is presented. The general solutions for beams with cosine loads are obtained in case of thick cantilever beams. The displacements and stresses obtained by present theory are in excellent agreement with those of other equivalent refined and higher order theories. The present theory yields the realistic variation of axial displacement and stresses through the thickness of beam. Thus the validity of the present theory is established.

REFERENCES

[1] J. A. C. Bresse, "Cours de Mechanique Applique", Mallet-Bachelier, Paris, 1859.
[2] J. W. S. Lord Rayleigh, "The Theory of Sound", Macmillan Publishers, London, 1877.
[3] S. P. Timoshenko, "On the correction for shear of the differential equation for transverse vibrations of prismatic bars", *Philosophical Magazine*, vol. 41, no. 6, pp. 742-746, 1921.
[4] G. R. Cowper, "The shear coefficients in Timoshenko beam theory", *ASME J. of Applied Mechanic*, vol. 33, no. 2, pp. 335-340, 1966.
[5] G. R. Cowper, "On the accuracy of Timoshenko beam theory", *ASCE J. of Engineering Mechanics Division*. Vol. 94, no. EM6, pp. 1447-1453, 1968.
[6] M. Levinson, "A new rectangular beam theory", *J. of Sound and Vibration*, vol. 74, no.1, pp. 81-87, 1981.
[7] W. B. Bickford, "A consistent higher order beam theory", *Int. Proceeding of Dev. in Theoretical and Applied Mechanics* (SECTAM), vol. 11, pp. 137-150, 1982.
[8] L. W. Rehfield, P. L. N. Murthy, "Toward a new engineering theory of bending: fundamentals", *AIAA J.* vol. 20, no. 5, pp. 693-699, 1982.
[9] A. V. Krishna Murty, "Towards a consistent beam theory", *AIAA J.*, vol. 22, no. 6, pp. 811-816, 1984.
[10] M. H. Baluch,, A. K. Azad, M. A. Khidir, "Technical theory of beams with normal strain", *ASCE J. of Engineering Mechanics*, vol. 110, no. 8, pp. 1233-1237, 1984.
[11] A. Bhimaraddi, K. Chandrashekhara, "Observations on higher order beam Theory", *ASCE J. of Aerospace Engineering*, vol. 6, no.4, pp. 408-413, 1993.
[12] H. Irretier, "Refined effects in beam theories and their influence on natural frequencies of beam", *Int. Proceeding of Euromech Colloquium*, 219, on Refined Dynamical Theories of Beam, Plates and Shells and Their Applications, Edited by I. Elishak off and H. Irretier ,Springer-Verlag, Berlin, pp. 163-179, 1986.
[13] T. Kant, A. Gupta, "A finite element model for higher order shears deformable beam theory*", J. of Sound and Vibration*, vol. 125, no. 2, pp. 193-202, 1988.
[14] P. R. Heyliger, J. N. Reddy, "A higher order beam finite element for bending and vibration problems", *J. of Sound and Vibration*, vol. 126, no. 2, pp. 309-326, 1988.
[15] R. C. Averill, J. N. Reddy, "An assessment of four-noded plate finite elements based on a generalized third order theory", *Int. J. of Numerical Methods in Engineering*, vol. 33, pp. 1553-1572, 1992.
[16] J. N. Reddy, "An Introduction to Finite Element Method". 2nd Ed., McGraw-Hill, Inc., New York, 1993.
[17] V. Z. Vlasov, U. N. Leont'ev, "Beams, Plates and Shells on Elastic Foundations" Moskva, Chapter 1, 1-8. Translated from the Russian by A. Barouch and T. Plez *Israel Program for Scientific Translation Ltd., Jerusalem*, 1966.
[18] M. Stein, "Vibration of beams and plate strips with three dimensional flexibility", *ASME J. of Applied Mechanics*, vol. 56, no. 1, pp. 228-231, 1989.
[19] Y. M. Ghugal. Y.M., R. Sharma, "A hyperbolic shear deformation theory for flexure and vibration of thick isotropic beams", *Int. J. of Computational Methods*, vol. 6, no. 4, pp. 585-604, 2009.
[20] Y. M. Ghugal, R. P. Shmipi, "A review of refined shear deformation theories for isotropic and anisotropic laminated beams", *J. of Reinforced Plastics and Composites*, vol. 20, no. 3, pp. 255-272, 2001.
[21] F. B. Hildebrand, E. C. Reissner, "Distribution of Stress in Built-In Beam of Narrow Rectangular Cross Section", *J. of Applied Mechanics,* vol. 64, pp. 109-116, 1942.